Journal of Alloys and Compounds 509 (2011) 5506–5514

Contents lists available at ScienceDirect

Journal of Alloys and Compounds

journal homepage: www.elsevier.com/locate/jallcom

Effect of boron on microstructure and mechanical properties of thermomechanically processed near alpha titanium alloy Ti-1100

V.K. Chandravanshi*, R. Sarkar, S.V. Kamat, T.K. Nandy

Defence Metallurgical Research Laboratory, Hyderabad 500058, Andhra Pradesh, India

ARTICLE INFO

Article history:
Received 11 November 2010
Received in revised form 15 February 2011
Accepted 21 February 2011
Available online 26 February 2011

Keywords:
Ti-1100 alloy
Boron
Mechanical properties
Thermomechanically processed

ABSTRACT

The effect of 0.2 wt.% of boron on the mechanical properties of Ti-1100, a near α titanium alloy, was evaluated at room temperature and at 600 °C in the as cast and thermomechanically processed (α–β rolled) condition after subjecting it to different heat treatments. Boron addition in Ti-1100 significantly refined the microstructure in the as cast condition but the mechanical properties did not show any improvement. However, in the thermomechanically processed (α–β rolled) and standard heat treatment condition, the yield strength (YS) and ultimate tensile strength (UTS) of the boron containing alloy increased significantly without any drop in elongation-to-failure as compared to the base alloy at both room temperature and 600 °C. No discernible trend was seen in YS and UTS in boron containing alloy with change in solution treatment temperature either at room temperature or at 600 °C.

1. Introduction

Titanium alloys are important aerospace materials for structural and engine applications because of their high strength to weight ratio and ability to withstand elevated temperatures up to 600 °C [1]. Many titanium alloy compositions and their microstructural design have been optimized over last six decades and additional improvements in mechanical properties have been continually sought. While the pace of conventional alloy development efforts have slowed down, alternative routes for improving major properties are being explored. Continuous fiber reinforced Ti-alloy matrix composites (TMCs) have been investigated extensively for high temperature applications [1]. While they exhibit outstanding properties in terms of stiffness, strength and creep, the high costs involved with fiber processing limit their widespread application. In addition, they suffer from internal residual stresses arising from thermal expansion mismatch between fibers and the matrix leading to property deterioration, notch sensitivity and multiple cracking of matrix during fatigue loading. Because of the above mentioned problems encountered in continuous fiber reinforced composites, attempts have also been made to explore particulate composites, Ti–B and Ti–C systems being the prime examples [2–5].

In recent times, conventional Ti alloys containing small amounts of boron (B) have been gaining considerable interest due to their attractive mechanical properties that include superior room-temperature (RT) specific stiffness, higher strength along with reasonable elongation-to-failure [6–9] and reasonably good low cycle fatigue properties [10–12]. The significant increase in strength and stiffness in Ti–B alloys arises from the presence of strong and stiff TiB whiskers that precipitate *in situ* during solidification [6,10,13]. Recent work has also shown that the addition of trace amounts (~0.1 wt.%) of B to Ti–6Al–4V decreases the as-cast grain size by approximately an order of magnitude [9,14,15] that facilitates the subsequent processing substantially [16,17]. While considerable work has been done on as cast titanium alloys (induction and vacuum arc melted), investigations on wrought boron modified alloys are limited. Previously, a detailed study on the effect of boron in vacuum arc melted Timetal 685 in the as cast condition showed rapid deterioration in elongation-to-failure with increasing boron content [18]. Additionally, it is well known that cast titanium alloys exhibit substantial scatter in mechanical properties. In the light of the above, property evaluation of boron-modified alloys in the thermomechanically processed condition is essential to realize the full potential of these alloys.

In the present investigation, the effect of 0.2 wt.% of boron on the mechanical properties of Ti-1100, a near α titanium alloy, was evaluated in the as cast and thermomechanically processed conditions. The heat treatments were also varied to study their effect on the mechanical properties of Ti-1100 and boron modified Ti-1100 alloys.

2. Experimental procedure

Nominal compositions of the Ti-1100 alloy with and without boron (melted using consumable vacuum arc melting) are shown in Table 1. O and N, reported

* Corresponding author. Tel.: +91 40 24586791.
E-mail addresses: vivekmet@dmrl.drdo.in, vivekmet@gmail.com (V.K. Chandravanshi).

0925-8388/$ – see front matter © 2011 Elsevier B.V. All rights reserved.
doi:10.1016/j.jallcom.2011.02.114

Table 1
Nominal composition (wt.%) of the alloys investigated.

Alloy	Al	Sn	Zr	Mo	Si	B	O[a]	N[a]	Ti
Ti-1100	6	2.75	4	0.4	0.45	0	1020 ppm	<20 ppm	Balance
Ti-1100 + 0.2B (Ti-1100B)	6	2.75	4	0.4	0.45	0.2	960 ppm	<20 ppm	Balance

[a] O and N are analysed.

in Table 1, were analysed by LECO™ gas analyzer. While Ti, Al, Zr, Si and B were added in elemental form, Mo was added as Mo/Al master alloy. The details of melting are provided in an earlier publication [18]. Slices were cut from the top and bottom for macrostructural examination. Beta transus temperatures (β_T) of the alloys were determined by solution treating specimens in the temperature range of 900–1050 °C followed by water quenching and examining the microstructure. The beta transus temperatures of the alloy with and without boron were found to be 1030 °C and 1015 °C, respectively. The increase in the beta transus temperature with boron addition is in accordance with earlier studies done by Soboyejo et al. [19] and Tamirisakandala et al. [20]. The ingots were forged at 1100 °C from 140 mm diameter to 30 mm thickness, in order to break the cast structure. Following this, rolling was done in α–β region for both Ti-1100 + 0.2B (Ti-1100B) and Ti-1100 base alloys.

A series of heat treatments, involving solution treatment and ageing, were employed for the evaluation of mechanical properties. Samples were given solution treatments at $\beta_T - 100$ °C (β_T = beta transus temperature), $\beta_T - 50$ °C, $\beta_T - 30$ °C, and $\beta_T + 10$ °C for 2 h, air cooled followed by a standard ageing treatment at 595 °C/8 h/AC. A standard heat treatment (1095 °C/2 h/air cool plus 595 °C/8 h/air cool) [21] was also carried out for both the alloys. A FEI Quanta 400 (Netherlands) environmental scanning electron microscope (ESEM) was used for the examination of microstructures and fracture surfaces of the failed specimens.

Tensile tests at room temperature and 600 °C were carried out as per ASTM standard [22] in a screw driven Instron testing machine (5500R) and in Walter Bai ag (w + b) testing machine respectively, at an initial strain rate of 6×10^{-4} s^{-1}. Two specimens were tested in each condition and the average value was reported. In the as cast condition where the microstructure is not uniform from periphery to center, enough care was taken to select specimens from similar locations that are near the center of the slice extracted from the middle of the ingot. For the high temperature tests, the specimens were heated in a split resistance furnace which is attached to the Walter Bai ag (w + b) testing machine and soaked for 30 min at the test temperature (600 °C) prior to the commencement of testing. In both the room temperature and high temperature tensile tests, the strains were measured using a 25 mm gauge length extensometer.

3. Results

3.1. Macrostructures and microstructures

Macrostructures of 140 mm diameter secondary ingots of both alloys are shown in Fig. 1. A coarse grain structure is observed in the base alloy Ti-1100. Two distinct regions are apparent: (a) region I comprising columnar grains emanating from the periphery to the center and (b) region II showing equiaxed grains. The structure is considerably refined in Ti-1100B (boron containing alloy) (Fig. 1b). The region of columnar grains observed in the base alloy is absent in the boron-containing alloy.

Distribution of TiB whiskers, from two different locations (top and bottom) of the as cast ingot of Ti-1100B, are shown in low magnification micrographs of Fig. 2a and b, respectively. The micrographs clearly point towards homogeneity in TiB distribution evidenced by similar volume fraction, 1.7 pct in the top and bottom of the as cast ingot. The volume fraction of TiB was determined using ImageJ image analysis software on optical micrographs. The micrographs also show that TiB whiskers are located in the interdendritic regions. The morphology of TiB whiskers in as cast plus heat-treated and rolled plus heat treated condition is shown in Fig. 3a and b, respectively. The difference in morphology of TiB whiskers is evident. While the cast structure shows thin and long TiB whiskers with high aspect ratio ($l = 47 \pm 23$ μm, $d = 3 \pm 1.5$ μm, aspect ratio = 18 ± 10), the whiskers in the rolled structure are considerably smaller in length with much lower aspect ratio ($l = 10.5 \pm 4.5$ μm, $d = 1.8 \pm 0.4$ μm, aspect ratio = 6 ± 1.5) As mentioned earlier, the whiskers that are located at interdendritic boundaries form cell like structures prior to rolling, however, after rolling, they tend to align along the rolling direction. Cracking of TiB whiskers after rolling is seen in Fig. 4. Microstructures of Ti-1100 in as processed (α–β rolling) and different heat treatment conditions are shown in Fig. 5. While the base alloy exhibits equiaxed or elongated α in transformed β matrix in α–β heat treatment conditions (Fig. 5a–c), a fully transformed β structure comprising acicular or martensitic α phase is seen in the β heat treatment condition (Fig. 5d). Microstructures of Ti-1100B in the α–β processed plus solution treatment ($\beta_T - 100$ °C, $\beta_T - 50$ °C, $\beta_T - 30$ °C, and $\beta_T + 10$ °C) and aged (595 °C/8 h/AC) conditions are shown in Fig. 6. While coarse and partially globularised α microstructures are seen in Fig. 6a–c where the heat-treatment has been carried out below β transus, a transformed β microstructure with finer α (with acicular morphology) structure is seen in β treated specimen (Fig. 6d). Prior beta grain sizes in fully transformed beta structure ($\beta_T + 10$ °C heat treatment) was measured by mean linear intercept method using a minimum of five frames. They were found to be 390 ± 50 μm and 115 ± 30 μm in Ti-1100 and Ti-1100B, respectively.

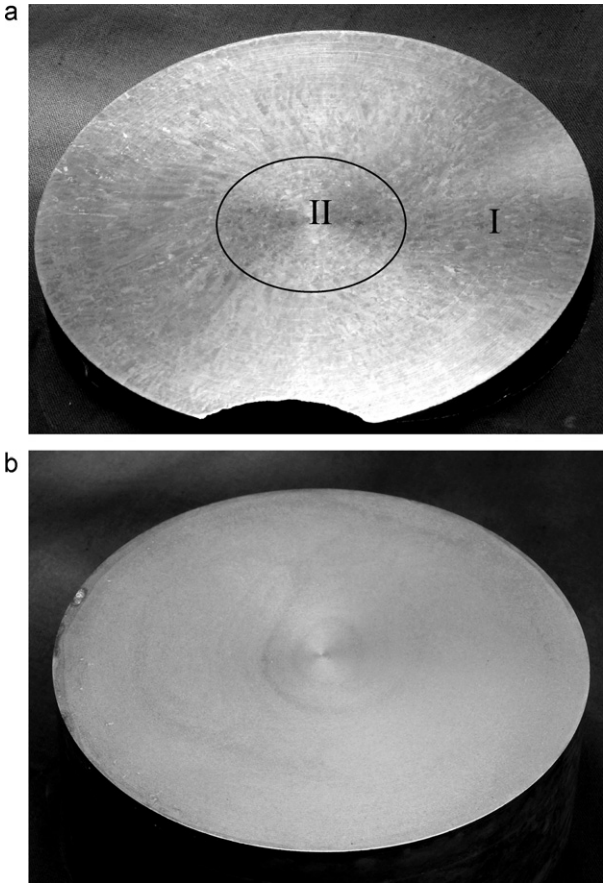

Fig. 1. Macrostructures: (a) Ti-1100 and (b) Ti-1100B. Coarse grain structure in Ti-1100 as compared to Ti-1100B is evident.

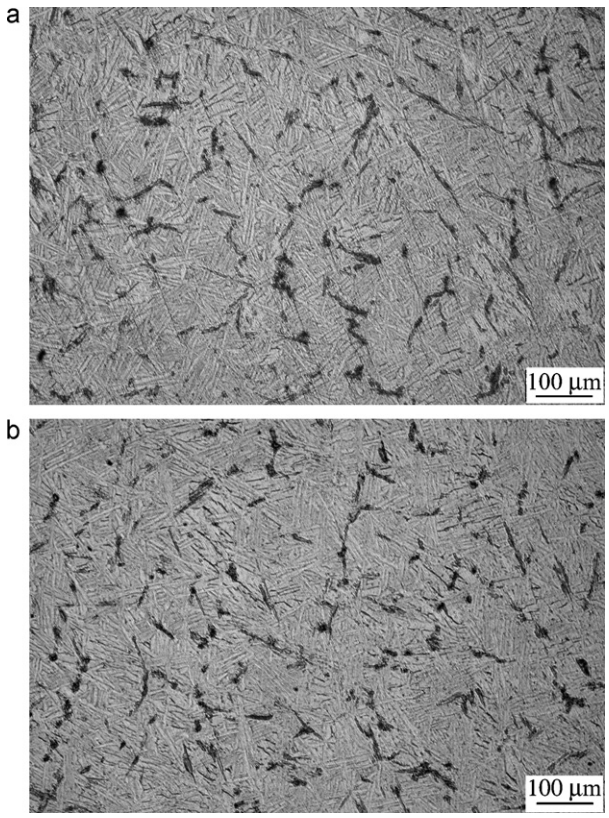

Fig. 2. Distribution of TiB whiskers in Ti alloy matrix: (a) top and (b) bottom.

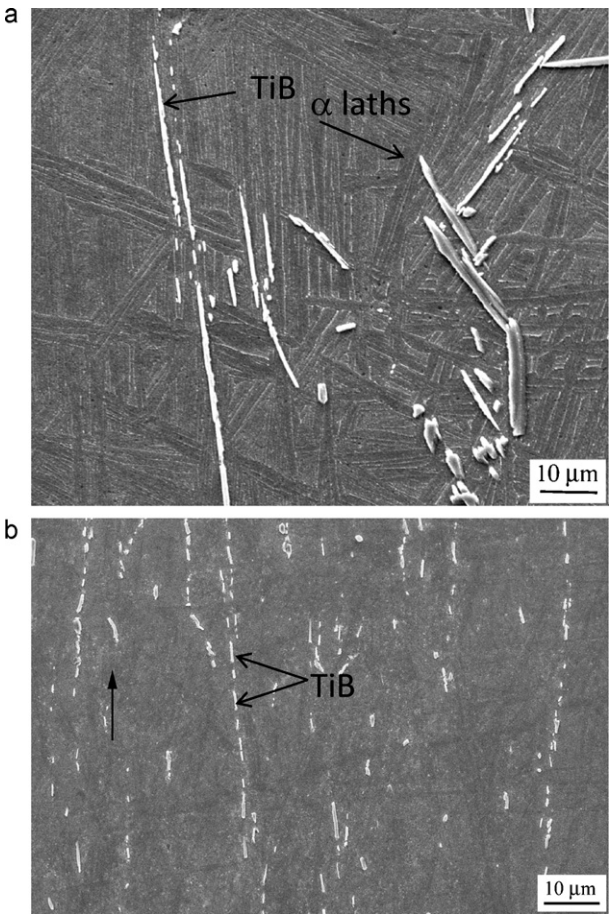

Fig. 3. Comparision of TiB whisker size and morphology (a) as cast + HT and (b) rolled + HT. Rolling direction is shown in (b).

3.2. Mechanical behaviour

Comparative room temperature tensile curves of cast and heat treated Ti-1100 and Ti-1100B along with those of processed alloys in a standard heat treatment condition are shown in Fig. 7. The results of the tensile properties of cast and processed alloys followed by a standard heat treatment are summarized in Table 2. In the boron-containing alloy (Ti-1100B), the strength increment in the as cast plus heat-treated condition as compared to Ti-1100 (as cast plus heat treated) is only marginal and degradation in elongation-to-failure in boron containing alloy is significant. However, in the thermomechanically processed and standard heat treatment condition, Ti-1100B shows a higher strength as compared to Ti-1100. Additionally, the processed boron containing alloy shows higher elongation-to-failure values as compared to the base alloy. The elastic modulus values of the boron containing alloy at room temperature are higher than the base alloy in all conditions.

As mentioned earlier a series of heat treatments at different solution treatment temperatures in processed condition were employed to generate a detailed heat-treatment, microstructure and tensile property data set at room temperature and 600 °C. Representative room temperature tensile curves of α–β and β heat treated samples are shown in Fig. 8a and b. The results of room temperature tensile property evaluation in various heat treatment conditions are summarized in Table 3. Ti-1100B alloy shows

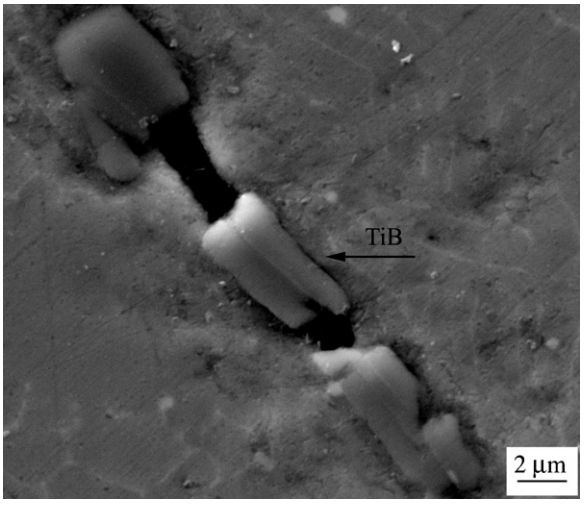

Fig. 4. Cracking in TiB whiskers in as rolled conditions (SE images): Ti-1100B (rolled at 980 °C).

Table 2
Room temperature tensile properties of cast and processed Ti-1100 and Ti-1100B in standard heat treatment condition (1095 °C/2 h/AC + 595 °C/8 h/AC).

Alloy designation	Processing condition	0.2% Y.S. (MPa)	UTS (MPa)	*E* (GPa)	% elongation to failure
Ti-1100	As cast	937	1050	112	3.9
Ti-1100B	As cast	938	1037	125	1.3
Ti-1100	(α–β rolled at 875 °C)	931	1027	114	3.0
Ti-1100B	(α–β rolled at 980 °C)	963	1112	128	7.5

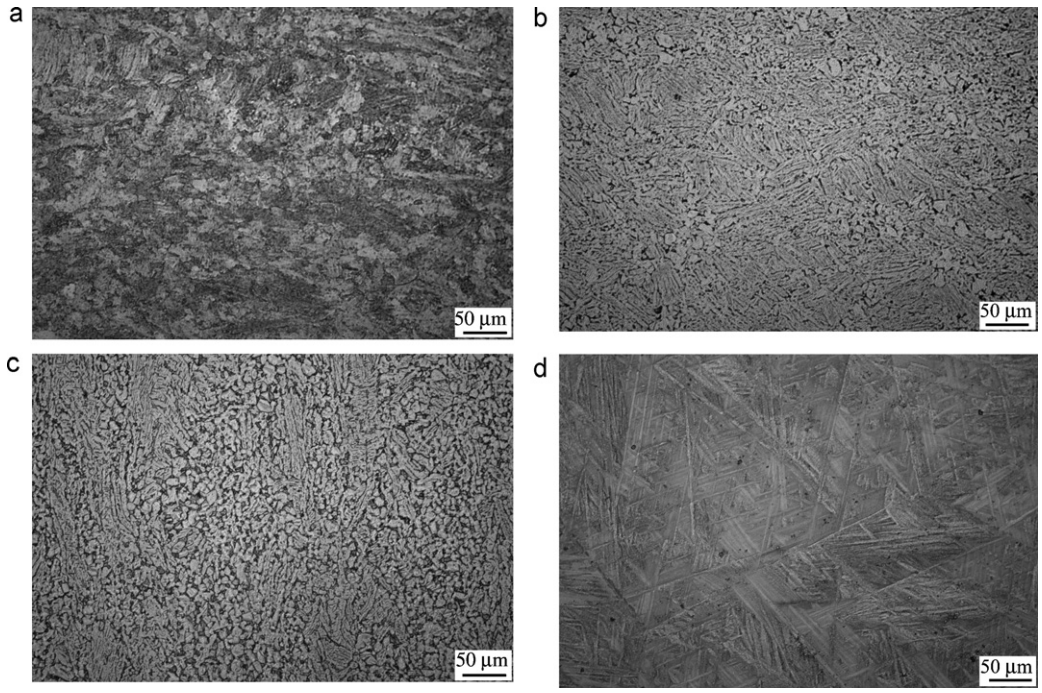

Fig. 5. Optical microstructures of Ti-1100 (a) HT at 915 °C/2 h/AC + 595 °C/8 h/AC, (b) 965 °C/2 h/AC + 595 °C/8 h/AC, (c) 985 °C/2 h/AC + 595 °C/8 h/AC, and (d) 1025 °C/2 h/AC + 595 °C/8 h/AC.

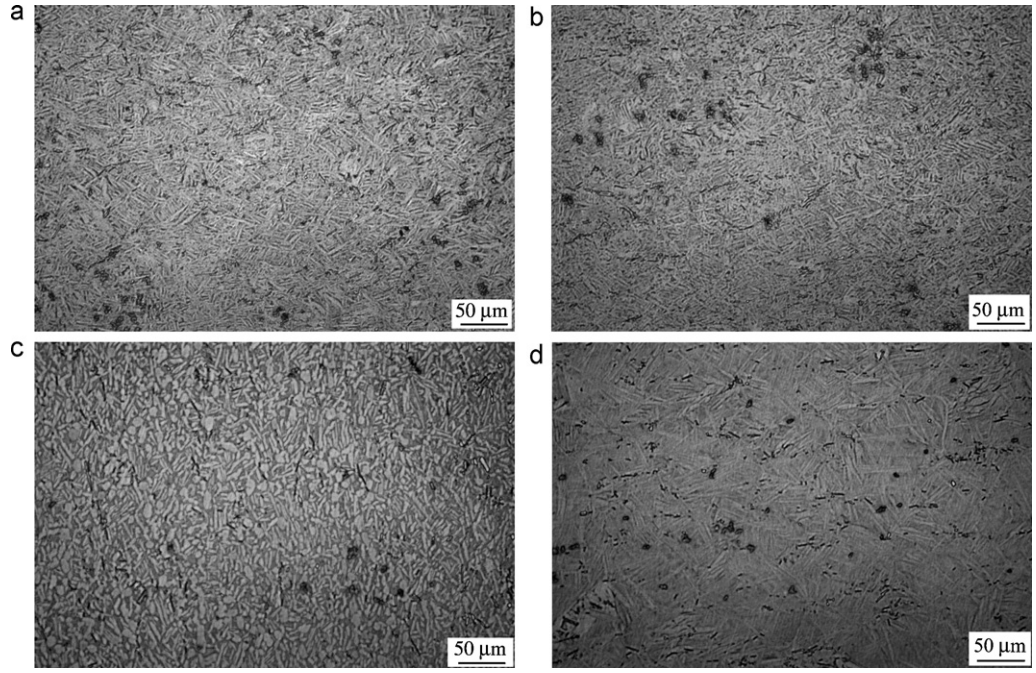

Fig. 6. Optical microstructures of Ti-1100B: (a) HT at 930 °C/2 h/AC + 595 °C/8 h/AC, (b) 980 °C/2 h/AC + 595 °C/8 h/AC, (c) 1000 °C/2 h/AC + 595 °C/8 h/AC, and (d) 1040 °C/2 h/AC + 595 °C/8 h/AC.

Table 3
Room temperature tensile properties of Ti-1100, and Ti-1100B (x °C/2 h/AC + 595 °C/8 h/AC).

Alloy designation	Solutionizing Temp (°C)	0.2% Y.S. (MPa)	UTS (MPa)	E (GPa)	% elongation to failure
Ti-1100	915 ($\beta_T - 100$ °C)	899	989	109	9.1
	965 ($\beta_T - 50$ °C)	948	1034	107	10.2
	985 ($\beta_T - 30$ °C)	931	1033	108	9.6
	1025 ($\beta_T + 10$ °C)	872	1026	114	6.7
Ti-1100B	930 ($\beta_T - 100$ °C)	1014	1150	129	7.9
	980 ($\beta_T - 50$ °C)	1015	1129	130	12.4
	1000 ($\beta_T - 30$ °C)	951	1082	125	11.8
	1040 ($\beta_T + 10$ °C)	946	1098	126	8.2

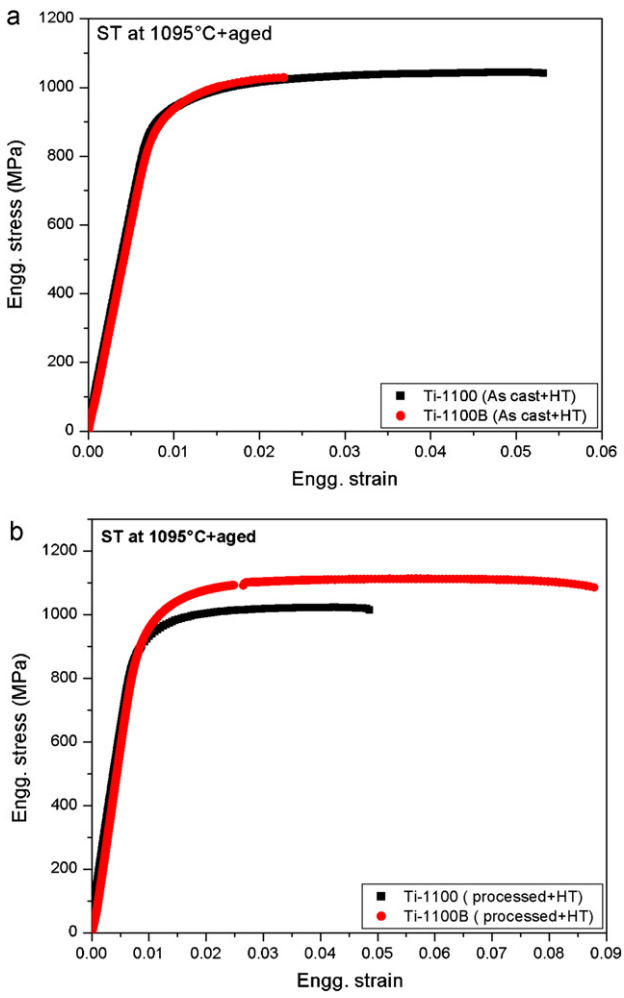

Fig. 7. Room temperature tensile properties of Ti-1100 and Ti-1100B in as cast + HT and processed + HT conditions.

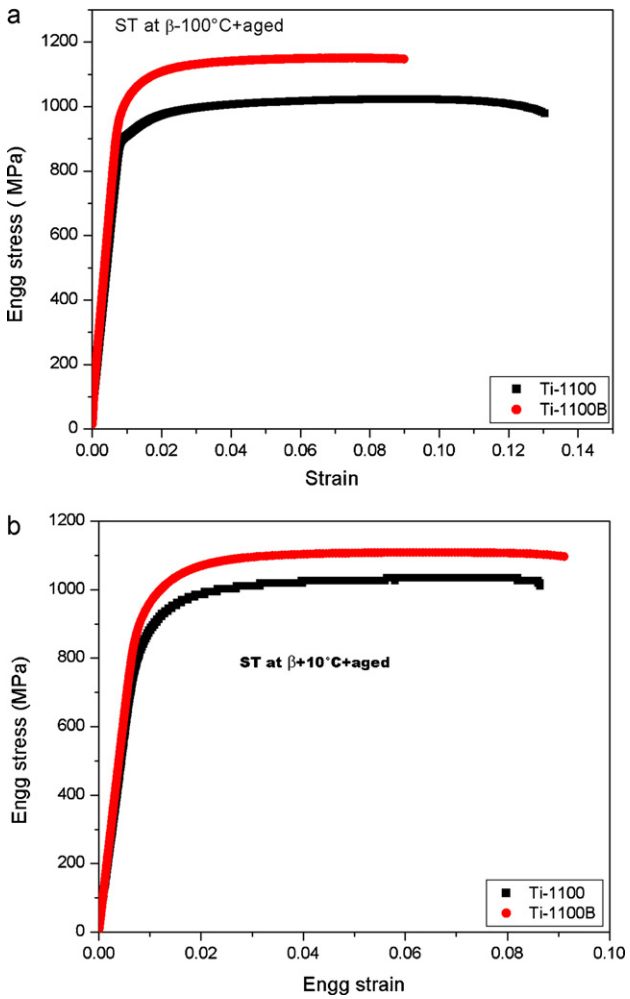

Fig. 8. Room temperature tensile properties of processed Ti-1100 and Ti-1100B at various STA conditions.

higher strength properties as compared to Ti-1100 with similar elongation-to-failure at room temperature. High temperature tensile property data are also listed in Table 4. Again, the boron containing alloy shows higher strength as compared to the base alloy for similar heat treatment conditions. The elongation-to-failure values of the alloys are comparable regardless of the heat treatment condition. As compared to room temperature, lowering of strength and increase in elongation-to-failure in all conditions for the two alloys are noticeable at high temperature.

Representative fractographs of room temperature failed tensile specimens in one of the α–β heat treated conditions are shown in Fig. 9 for both the base and the boron containing alloy. The base as well as the boron containing alloy show the presence of dimples on the fracture surface (although the dimples appear to be shallower in the boron containing alloy) indicating that the microscopic mechanism of fracture is ductile in both cases. Longitudinal sections of tensile tested specimens are shown in Fig. 10. In the base alloy, cracking appears to originate from the transformed β region whereas in the boron containing alloy, the cracking is observed in TiB precipitates. While frequent cracking is observed in TiB precipitates, occasionally decohesion along TiB–Ti interface is also visible.

4. Discussion

4.1. Microstructure

The observation of finer macro (Fig. 1) and microstructure (Fig. 2) in the as cast Ti-1100B alloy as compared to that in the as cast matrix alloy (Ti-1100) is consistent with the reported literature in a variety of alloy systems. Alloys such as Ti-6-4 [9,14], Ti-6-2-4-2

Table 4
High temperature (600 °C) tensile properties of Ti-1100, and Ti-1100B (x °C/2 h/AC + 595 °C/8 h/AC).

Alloy designation	Solutionizing temp (°C)	0.2% Y.S. (MPa)	UTS (MPa)	% elongation to failure
Ti-1100	915	513	640	23.3
	965	526	644	17.7
	985	513	636	21.6
	1025	537	695	14.1
Ti-1100B	930	545	634	12.7
	980	547	683	15.3
	1000	571	711	12.0
	1040	594	730	12.1

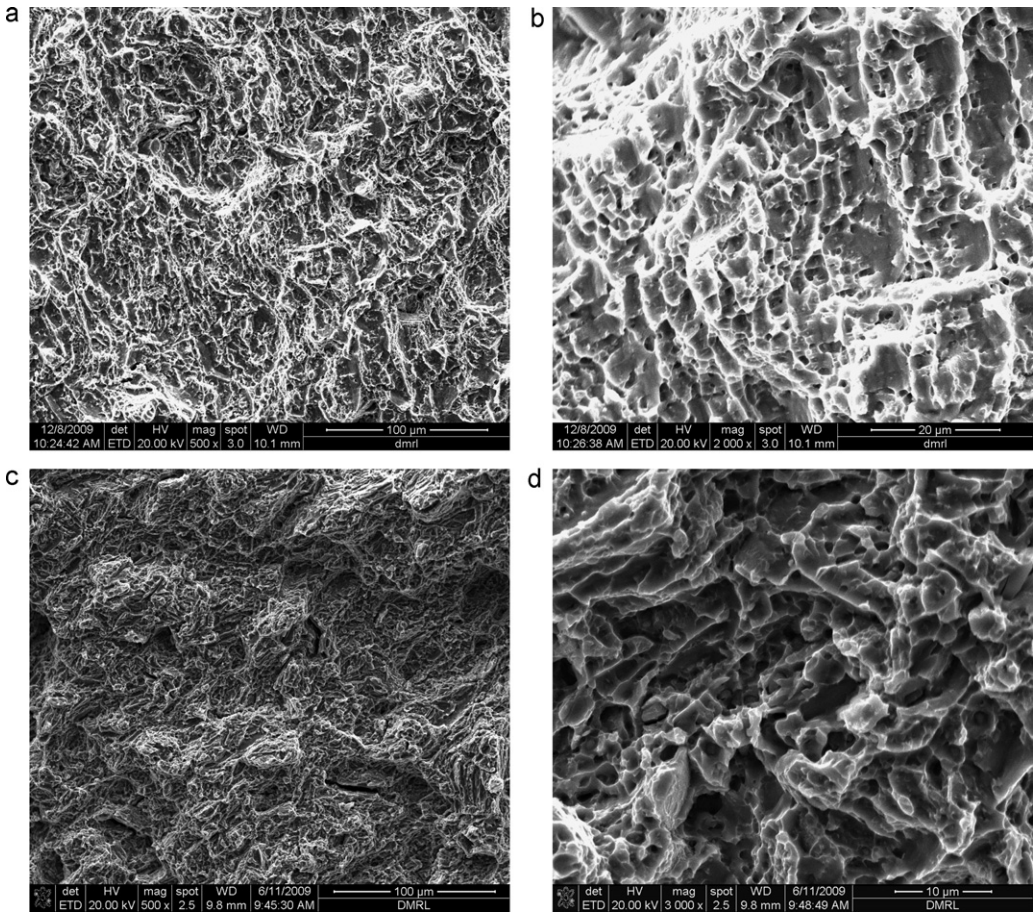

Fig. 9. Fractographs (β_T − 100 °C/2 h/AC + 595 °C/8 h/AC): (a) and (b) Ti-1100; (c) and (d) Ti-1100B.

[14], Ti-21S [15], Ti-5-5-5-3 [15], Timetal 685 [18] and also pure Ti [23] have shown refinement in microstructure (especially prior β grain size) with addition of boron. This has been attributed to constitutional supercooling caused by the presence of boron [24]. As the β phase nucleates, it rejects boron into the liquid. This leads to solute enrichment in the liquid ahead of the solid–liquid interface resulting in constitutional supercooling leading to instability in solid–liquid interface and formation of more nuclei. Once nuclei are formed, the presence of boron rich layer retards the grain growth allowing more grains to form in the surrounding area. This theory has also been supported by the observation of an excellent correlation between grain size and growth restriction factor (Q) in the boron containing titanium alloy Ti-6-2-4-2 [14].

Figs. 3 and 4 also show that the TiB whiskers crack and fragment into smaller whiskers after thermomechanical processing. This has also been reported in boron containing Ti–6Al–4V alloys by Srinivasan et al. [16,17]. While the aspect ratio of TiB whiskers in the as cast condition is 18 ± 10, it is 6 ± 1.5 in the thermomechanically processed condition. TiB being an intermetallic has limited elongation-to-failure and the whiskers formed during solidification also have statistically distributed flaws within them [25]. During thermomechanical processing, the strain incompatibility between the relatively ductile matrix alloy and the undeformable TiB whiskers cause the whiskers to fragment because of the propagation of the flaws. The whiskers also tend to align along the rolling direction [16] after thermomechanical processing. Similar observation has also been reported by Srinivasan et al. [16,17] in as processed Ti–6Al–4V–0.1B alloy.

Figs. 5 and 6 shows that both the base and boron containing alloy show equiaxed or partially elongated α in a transformed β matrix in the α–β rolled and heat treated condition. This is expected as the processing of the alloy in the two phase region results in the fragmentation of α brought about by the pinching of β and rotation of α phase [26,27]. On the other hand, these figures also show that both the base and boron containing alloy exhibit a fully transformed β structure with lenticular α morphology following β heat treatment. Thus it appears while boron influences the microstructure of as cast Ti-1100 alloy, it does not significantly affect the microstructure in thermomechanically processed condition. The microstructure in processed and heat treatment condition depends upon the rolling and heat treatment temperatures.

4.2. Mechanical behaviour

Higher elastic modulus of the boron containing alloy in different heat treatment conditions as compared to the base alloy is consistently observed. This is consistent with the results obtained by Sen et al. [9] in Ti–6Al–4V alloy and Tamirisakandala et al. [15] in Ti-21S and Ti-5-5-5-3 alloys. This may be attributed to the presence of TiB whiskers which has significantly higher elastic modulus than the matrix [2]. Table 2 clearly shows that there is no change in the strength and a reduction in elongation-to-failure on addition of 0.2 wt.% B in the Ti-1100 alloy in the as cast condition. A similar behaviour was also observed in the Ti-685 alloy [18]. On the other hand, both the strength and elongation-to-failure increase with addition of 0.2 wt.% B in the Ti-1100 alloy in the thermomechanically processed and heat treated condition. The behaviour in the as cast condition is attributed to the random distribution of the whiskers as well as the brittle nature of the matrix. The random distribution of whiskers does not result in an efficient transfer of

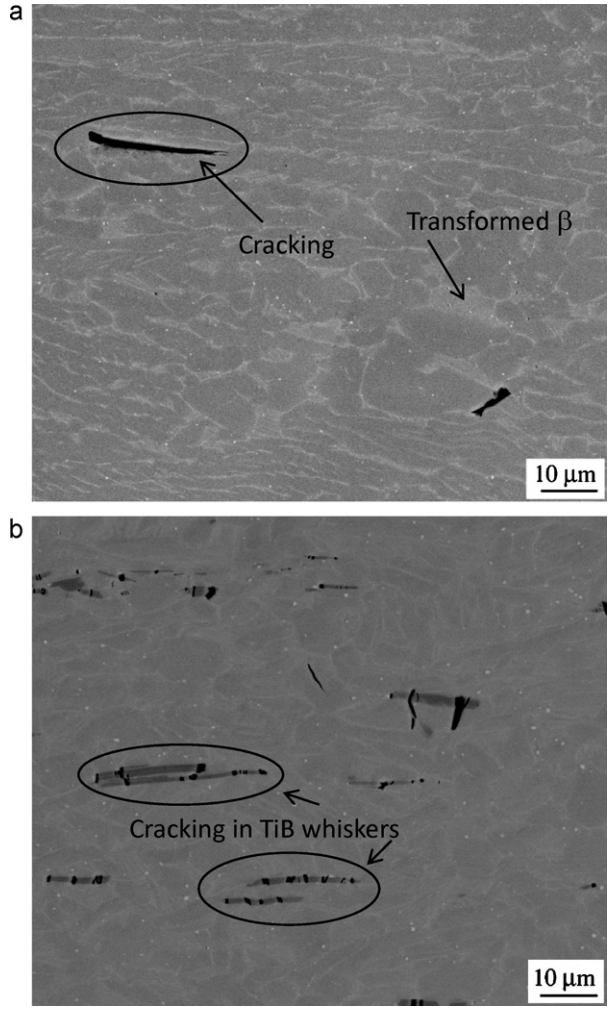

Fig. 10. Longitudinal section (BSE images) ($\beta_T - 30\,^\circ$C/2 h/AC + 595 °C/8 h/AC): (a) cracking in Ti-1100 in transformed beta region and (b) cracking in TiB whiskers (Ti-1100B).

loads to the whiskers. Also, the matrix because of its having high Al equivalent and coarse grain size is brittle and its failure occurs much before the whiskers reach their failure strains. Hence the full benefit of whisker strengthening is not experienced by the material. The results are in contrast to those reported in as cast boron modified Ti–6Al–4V alloys [9] where the matrix, which has lower Al equivalent (~6 as compared to ~7.6 in Ti-1100) is relatively more ductile.

As mentioned earlier, the TiB whiskers tend to fragment and align along the rolling direction during thermomechanical processing. Thus, to understand the mechanical behaviour of the boron containing Ti-1100 alloys in the thermomechanically processed condition we may consider it as metal matrix composite with aligned but initially fragmented whiskers. A similar approach has been used by Boehlert et al. [25] who have used an existing theory for deformation and fracture of a metal matrix composite with aligned but initially fragmented fibers proposed by Curtin and Zhou [28] to predict the strength of TiB whiskers as well as to rationalize the mechanical properties in Ti–6Al–4V–1B alloys. In this theory, the whiskers are loaded in tension through the shear stresses along well bonded matrix/whisker interfaces. The whiskers then undergo damage during tensile loading due to the statistically distributed flaws in the whiskers, with the matrix yielding along the lateral sides of the whiskers around the break points. Boehlert et al. [25] predict an approximate but analytic stress–strain curve for such a composite to be given by:

$$\sigma = f\sigma_c \left(\frac{1}{\rho}\right)(1 - e^{-\rho T}) + (1 - f)\sigma_m(\varepsilon) \quad (1)$$

where, $\sigma_c = (\sigma_0^m \tau L_0/r)^{1/m+1}$ is the characteristic whisker strength, $T = E\varepsilon/\sigma_c$ is the dimensionless composite strain, $\rho = (\delta_c/L + T^m)$ is the dimensionless whisker damage parameter, $\delta_c = r\sigma_c/\tau$ is the characteristic or critical whisker length, f = volume fraction of TiB, r = radius of whisker, L = average length of whiskers, τ = matrix shear strength, E = elastic modulus, $\sigma_m(\varepsilon)$ = strength of matrix, and m = Weibull modulus.

The initial whisker length thus appears only as a part of the damage parameter ρ and corresponds to an initial amount of whisker damage at zero strain. For materials with limited work hardening, Boehlert et al. [25] have simplified the above equation and suggested that the ultimate tensile strength (UTS) of the composite can be expressed as:

$$\sigma_{uts} = f\sigma_c\xi(\rho_0, m) + (1 - f)\sigma_m(\varepsilon_{uts}) \quad (2)$$

where, $\xi(\rho_0, m)$ is a numerical factor that depends only on the dimensionless initial whisker length $\rho_0 = \delta_c/L = r\sigma_c/L\tau$ and the Weibull modulus m.

Eq. (2) thus relates the composite tensile strength, initial whisker length, matrix strength and characteristic whisker strength distribution. Boehlert et al. [25] have indirectly estimated that the *in situ* TiB whisker strength (σ_c) is 8.0 GPa with a Weibull modulus $m = 2$. If one assumes the same strength characteristics for the TiB whiskers in the present study and substitute the other parameters measured experimentally such as $r = 1.13$ μm, $L = 13.32$ μm, $f = 0.017$ (see Section 3), $\tau = \sigma_m/\sqrt{3} = 593$ MPa, $\sigma_m(\varepsilon_{uts}) = 1027$ MPa, $\rho_0 = \delta_c/L = r\,\sigma_c/L\tau = 1.12$ as well as $\gamma(m) = 1.975$ from [25], the ultimate tensile strength predicted for the present boron containing alloy in the standard heat treatment condition is 1072 MPa which is in reasonable agreement with the experimental value of 1112 MPa. The retention of high elongation-to-failure in the B containing alloy in the thermomechanically processed condition also can be explained on the basis of the above model. The analysis of Boehlert et al. [25] suggests that the elongation-to-failure is very sensitive to the whisker strength statistics and the initial whisker length relative to the critical length, i.e. $\rho_0 = \delta_c/L$. The high elongation to failure is obtained as long as ρ_0 is greater than a critical value ρ_0^* which for TiB whiskers with a strength of 8 GPa and Weibull modulus of 2 is ~0.5. In the present boron containing alloy $\rho_0 = \delta_c/L = 1.12$ is well above ρ_0^* and hence the high observed elongation-to-failure is also consistent with the predictions of the above model.

There is no discernible trend in the variation of yield strength and UTS in boron containing Ti-1100B alloy with change in heat treatment (i.e. solution treatment condition) although it broadly follows the change in the matrix yield and UTS (Fig. 11 and Table 3). This is consistent with the model as the change in the solution treatment temperature does not affect the whisker strength and damage characteristics but only changes the matrix strength because of the change in size and volume fraction of primary α and size of α in transformed β as well as the prior β grain size (in the case of solution treatment above β transus temperature). The retention of high elongation-to-failure in all the heat treatments can also be attributed to the fact that ρ_0 in all cases is well above ρ_0^* as the change in the strength values of the matrix is not that significant with the change in the heat treatment.

The yield strength and UTS of both the matrix as well as 0.2 wt.% B containing alloy decrease significantly at 600 °C as compared to room temperature for all heat treatment conditions (Table 4). However, like at room temperature, the boron containing alloy show a higher yield and ultimate tensile strength than the matrix alloys

Table 5
Comparison of room temperature tensile properties of boron modified titanium alloys.

Alloy designation	Condition	0.2% Y.S. (MPa)	UTS (MPa)	*E* (GPa)	% elongation-to-failure
Ti-64 [9]	Cast + HIP	834	900	107	6.0
Ti-64–0.1B	Cast + HIP	900	965	116	7.3
Ti-64–0.4B	Cast + HIP	913	972	126	5.2
Beta-21S [15]	Cast + HIP	944	965	89	2.3
Beta-21S + 0.1B	Cast + HIP	951	963	92	5.5
Ti-5553 [15]	Cast + HIP	996	1071	105	8.4
Ti-5553 + 0.1B	Cast + HIP	1033	1112	112	6.0
IMI685 [18]	Cast + STA[a]	826	920	–	5.0
IMI685 + 0.2B	Cast + STA	828	917	–	2.5
IMI685 + 0.5B	Cast + STA	850	864	–	0.3

[a] STA, solution treatment plus ageing.

at 600 °C for all heat treatments in the thermomechanically processed condition. The behaviour of the TiB whiskers is not expected to be significantly different at 600 °C and the effect of temperature will most likely depend on the mechanical properties of the base alloy. This is confirmed by the fact that the fall in the yield strength and UTS with temperature in the boron containing alloy is comparable to the fall in these properties of the base alloy. It is to be noted that the decrease in strength in the β heat treatment condition ($\beta_T + 10$ °C) is relatively low as compared to α–β heat treatment (such as $\beta_T - 100$ °C) conditions in both the alloys. This is expected since β heat treatment condition shows superior elevated temperature properties (such as tensile strength and creep) compared to α–β heat treatment condition [1]. The elongation-to-failure at elevated temperature in both the base and boron containing alloys are higher than those at room temperature. However, at elevated temperature, the boron containing alloys exhibit lower elongation-to-failure than the base alloy. This is in contrast to room temperature data where the elongation-to-failure values in the boron containing alloys are comparable or slightly higher than those of the base alloy.

Table 5 comprises the tensile test data generated by previous works on boron containing titanium alloys. While the previous results are mostly in cast + HIP or cast + solution treated and aged conditions, the present data is in wrought and heat treated conditions. It can be observed that much higher strength and elongation-to-failure are observed in the present study as compared to the previous investigations and this can be attributed to the present alloys being subjected to thermomechanical processing.

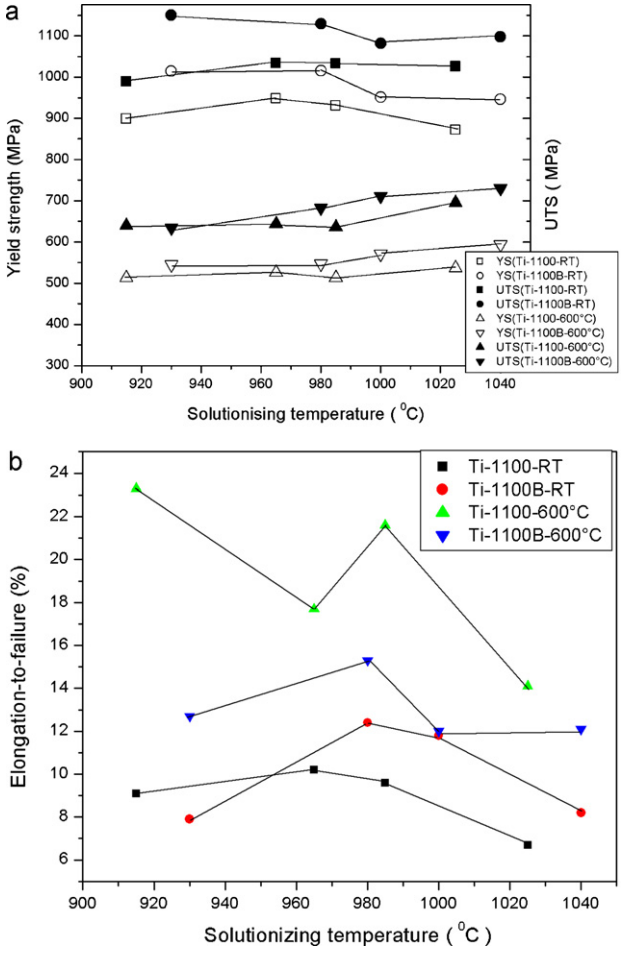

Fig. 11. Variation of tensile properties with solutionizing temperature: (a) yield strength and UTS and (b) elongation.

5. Conclusions

(a) No improvement in mechanical properties were found on addition of 0.2 wt.% boron in Ti-1100 alloy in the as cast condition even though there was significant refinement in the microstructure.
(b) Ti-1100 alloy with 0.2 wt.% boron exhibited a higher yield strength and ultimate tensile strength as compared to the base alloy at room temperature in the thermomechanically (α–β rolled) and standard heat treatment condition. The results were in-line with the predictions of a model based on treating the material as a metal matrix composite with aligned but fragmented whiskers.
(c) No discernible trends were observed in the variation of yield strength and UTS in boron modified Ti-1100 alloy with change in heat treatment (i.e. solution treatment condition) either at room temperature or at 600 °C although they broadly follow the change in the matrix yield strength and UTS.
(d) The strength properties of the Ti-1100 alloy with 0.2 wt.% boron in different heat treatment conditions were also found to be higher than those of the base alloy at 600 °C.
(e) The elongations-to-failure of the boron modified alloy in different heat treatment conditions were also found to be comparable or higher than those of the base alloy at room temperature. However, there was a marked degradation in the elongation to failure values in the boron modified alloy as compared to the base at 600 °C, although the elongation to failure values in both cases were higher than those at room temperature.

Acknowledgements

The authors are thankful to DRDO for funding this research activity. The authors are also thankful to Director, DMRL, Dr. G. Malakondaiah for his constant encouragement and permission to publish this work. The authors heartily acknowledge the suggestions given by Dr. A.K. Gogia.

References

[1] C. Leyns, M. Peters (Eds.), Titanium and Titanium Alloys, Wiley-VCH GmbH & Co. KGaA, Weinheim, 2003.
[2] K.S. Ravi Chandran, K.B. Panda, S.S. Sahay, JOM 56 (2004) 42–53.
[3] W.J. Lu, D. Zhang, X.N. Zhang, R.J. Wu, T. Sakata, H. Mori, Mater. Sci. Eng. A 311 (2001) 142–150.
[4] M.-M. Wang, W.-J. Lu, J. Qin, F. Ma, J. Lu, D. Zhang, Mater. Des. 27 (2006) 494–498.
[5] M.-M. Wang, W.-J. Lu, J. Qin, D. Zhang, B. Ji, F. Zhu, Scripta Mater. 54 (2006) 1955–1959.
[6] C.J. Boehlert, C.J. Cowen, S. Tamirisakandala, D.J. McEldowney, D.B. Miracle, Scripta Mater. 55 (2006) 465–468.
[7] C.J. Boehlert, Mater. Sci. Eng. A 510–511 (2009) 434–439.
[8] I. Sen, U. Ramamurty, Scripta Mater. 62 (2010) 37–40.
[9] I. Sen, S. Tamirisakandala, D.B. Miracle, U. Ramamurthy, Acta Mater. 55 (2007) 4983–4993.
[10] W. Chen, C.J. Boehlert, Mater. Sci. Eng. A 494 (2008) 132–138.
[11] W. Chen, C.J. Boehlert, E.A. Payzant, J.Y. Howe, Int. J. Fat 32 (2010) 627–638.
[12] W. Chen, C.J. Boehlert, Int. J. Fat 32 (2010) 799–807.
[13] W. Chen, C.J. Boehlert, Metall. Mater. Trans. A 40A (2009) 1568–1578.
[14] S. Tamirisakandala, R.B. Bhat, J.S. Tiley, D.B. Miracle, Scripta Mater. 53 (2005) 1421–1426.
[15] S. Tamirisakandala, R.B. Bhat, J.S. Tiley, D.B. Miracle, J. Mater. Eng. Perform. 14 (2005) 741–746.
[16] R. Srinivasan, D. Miracle, S. Tamirisakandala, Mater. Sci. Eng. A 487 (2008) 541–551.
[17] R. Srinivasan, D. Miracle, S. Tamirisakandala, K. Yu, V. Sinha, F. Sun, M. Bennett, J.M. Scott, M. Ninomi, S. Akiyama, M. Ikeda, M. Hagiwara, K. Maruyama (Eds.), Titanium Science and Technology, The Japan Institute of Metals, 2007, pp. 977–980.
[18] V.K. Chandravanshi, R. Sarkar, P. Ghosal, S.V. Kamat, T.K. Nandy, Metall. Mater. Trans. A 41 (2010) 936–946.
[19] W.O. Soboyejo, R.J. Lederich, S.M.L. Sastry, Acta Metall. Mater. 42 (1994) 2579–2591.
[20] S. Tamirisakandala, R.B. Bhat, D.B. Miracle, S. Boddapati, R. Bordia, R. Vanover, V.K. Vasudevan, Scripta Mater. 53 (2005) 217–222.
[21] R. Boyer, G. Welsch, E.W. Collings (Eds.), Materials Properties Handbook: Titanium alloys, 1994, pp. 411–414.
[22] ASTM E-8M, Annual Book of ASTM Standards, American Society of Testing and Materials, ASM International, Philadelphia, PA, 3.01, 2004, p. 62.
[23] M.J. Bermingham, S.D. McDonald, K. Nogita, D.H.St. John, M.S. Dargush, Scripta Mater. 59 (2008) 538–541.
[24] T.T. Cheng, Intermetallics 8 (2000) 29–37.
[25] C.J. Boehlert, S. Tamirisakandala, W.A. Curtin, D.B. Miracle, Scripta Mater. 61 (2009) 245–248.
[26] S.L. Semiatin, V. Seetharaman, I. Weiss, in: I. Weiss, R. Srinivasan, P.J. Bania, D. Eylon, S.L. Semiatin (Eds.), Advances in the Science and Technology of Titanium Alloy Processing, TMS, 1997, pp. 3–73.
[27] T.K. Nandy, A. Bhatterjee, A.K. Singh, A.K. Gogia, Met. Mater. Process. 18 (2006) 289–308.
[28] W.A. Curtin, S.J. Zhou, J. Mech. Phys. Solids 43 (1995) 343.